

# **Plasma-enhanced chemical vapor deposition of intrinsic microcrystalline silicon from chlorine-containing source gas**

R. Platz and S. Wagner

Princeton University, Department of Electrical Engineering, Princeton NJ 08544, USA

## **Abstract**

Microcrystalline silicon ( $\mu\text{c-Si:H}$ ) of truly intrinsic character can be deposited by plasma-enhanced chemical vapor deposition (PECVD) when dichlorosilane ( $\text{SiH}_2\text{Cl}_2$ ) is added to the  $\text{SiH}_4\text{-H}_2$  source gas. A dark-conductivity of  $5 \cdot 10^{-8}$  S/cm, activation energy of 0.62 eV and photo-conductivity of  $1 \cdot 10^{-5}$  S/cm are obtained. The optical bandgap for this material is approximately 1.1 eV. No special gas purification or microdoping is required.  $\text{SiH}_2\text{Cl}_2$  added in small amounts has the additional effects of enhancing the crystallinity, and of reducing the oxygen incorporation by over a factor of two. Sub-bandgap absorption spectroscopy indicates a low defect density. VHF deposition yields material with lower defect density and higher photo-conductivity than material deposited using DC plasma excitation. Transition from amorphous to microcrystalline growth occurs during the first 100-150 nm of film growth. The oxygen content increases as the crystallinity increases. A first p-i-n solar cell with a 1.8  $\mu\text{m}$  thick  $\mu\text{c-Si:H}(\text{:Cl})$  i-layer exhibits  $V_{\text{oc}} = 0.35$  V,  $I_{\text{sc}} = 4.14$  mA/cm<sup>2</sup> and FF = 55 %, demonstrating device-quality material.

## Introduction

Microcrystalline silicon ( $\mu\text{c-Si:H}$ ) is a form of thin-film silicon which is of growing interest for device applications. P-i-n solar cells incorporating  $\mu\text{c-Si:H}$  as the absorbing layer produce high photo-current and are stable against light-soaking<sup>1-3</sup>. Thin-film transistors (TFTs) with  $\mu\text{c-Si:H}$  channel layers have higher on-currents than amorphous silicon TFTs<sup>4-6</sup>.

$\mu\text{c-Si:H}$  is deposited at substrate temperatures of 200-300°C from highly  $\text{H}_2$  diluted silane ( $\text{SiH}_4$ ) by PECVD. Because of oxygen contamination<sup>7,8</sup>  $\mu\text{c-Si:H}$  is strongly n-type when deposited without special precautions. These donors reduce the electric field in part of the i-layer in a solar cell and thereby reduce the photocurrent collection efficiency. In a TFT, the unwanted oxygen doping causes undesirably high off-currents.

The oxygen donors can be compensated with boron at the ppm level ("microdoping"<sup>1,9,10</sup>). The need to tailor the boron doping to the case-by-case oxygen contamination and to control the doping within a very narrow window renders this method unsuitable for industrial practice. Truly intrinsic  $\mu\text{c-Si:H}$  has been obtained recently by purifying the gas with an oxygen getter and by carefully controlling the reactor condition<sup>8</sup>. A more robust deposition process which does not require additional equipment would be desirable for the production of  $\mu\text{c-Si:H}$  on an industrial scale.

In the present paper, we present a method for obtaining device-grade  $\mu\text{c-Si:H}$  by PECVD from  $\text{SiH}_4$  and  $\text{SiH}_2\text{Cl}_2$  diluted in  $\text{H}_2$ . Intrinsic material is deposited without any further measure and the growth process is very tolerant to changes in reactor conditions. Microcrystalline silicon using  $\text{SiH}_2\text{Cl}_2$  as a precursor gas has been deposited at several laboratories<sup>11-13</sup>, however without focussing on intrinsic material suitable for device-applications.

## Experiment

All samples were deposited from  $\text{SiH}_4$ ,  $\text{SiH}_2\text{Cl}_2$  and  $\text{H}_2$  at a substrate temperature of  $210^\circ\text{C}$ , unless otherwise stated. The depositions were performed in a conventional three-chamber system with load-lock using DC plasma excitation. One sample and the solar cell were prepared using very high frequency (VHF) plasma excitation at 70 MHz at otherwise identical deposition conditions. The hydrogen dilution ratio  $\text{H}_2/(\text{SiH}_4+\text{SiH}_2\text{Cl}_2)$  was kept constant at a value of  $\sim 35$ . Pressure during deposition was 0.9 torr. No special precautions were taken concerning the state of the reactor, such as pre-baking to reduce out-gassing from the walls. After  $\sim 30$  min. heating in the load-lock, the substrates were transferred to the deposition chamber, followed by deposition. The base pressure before deposition was  $\sim 1 \cdot 10^{-6}$  torr.

$\sigma_d$  and  $\sigma_{ph}$  were measured under vacuum using thermally evaporated Al contacts of 7.5 mm length and 0.5 mm spacing. The temperature-dependence of  $\sigma_d$  was used to determine  $E_{act}$ . Photo-conductivity was measured using homogeneously absorbed light of  $\lambda = 650$  nm wavelength and varying intensity;  $\sigma_{ph}$  values given in the text were obtained by extrapolation to a generation rate of  $10^{21} \text{ cm}^{-3}\text{s}^{-1}$ . A pronounced peak in the ultraviolet reflection spectrum at  $\sim 275$  nm is a reliable indication for microcrystalline material<sup>14,15</sup>. We therefore measured reflection spectra between 200 and 400 nm and determined the height of the 275 nm peak as an indication of the crystallinity of the material. The optical absorption coefficient in the high-energy region was determined using UV/visible transmission spectra and following the procedure proposed by Swanepoel<sup>16</sup>. Sub-bandgap absorption spectra were measured using the constant photo-current method (CPM) on samples with the same contact geometry as for the conductivity measurements. The I-V curve of the solar cell was measured at  $\sim 25^\circ\text{C}$  using light of  $100 \text{ mW/cm}^2$  intensity and a spectrum close to AM 1.5.

## Results

### *μc-Si:H deposited with SiH<sub>2</sub>Cl<sub>2</sub>*

Varying the SiH<sub>2</sub>Cl<sub>2</sub>/(SiH<sub>2</sub>Cl<sub>2</sub>+SiH<sub>4</sub>) ratio in the plasma between zero (pure H<sub>2</sub>-diluted SiH<sub>4</sub>) and one (pure H<sub>2</sub>-diluted SiH<sub>2</sub>Cl<sub>2</sub>) resulted in the dark-conductivity  $\sigma_d$ , dark-conductivity activation energy  $E_{act}$  and photo-conductivity  $\sigma_{ph}$  values of Figure 1, for ~500 nm thick films. The  $\mu c$ -Si:H sample deposited from pure H<sub>2</sub> diluted SiH<sub>4</sub> exhibits a high  $\sigma_d$  in excess of  $10^{-3}$  S/cm.  $E_{act}$  is <0.2 eV, reflecting high-level oxygen doping. Adding only a few percent of SiH<sub>2</sub>Cl<sub>2</sub> reduces  $\sigma_d$  by over five orders of magnitude to  $1.6 \cdot 10^{-8}$  S/cm, which is as low as the value obtained for  $\mu c$ -Si:H made by the microdoping or purifying techniques<sup>8,9</sup>.  $E_{act}$  is 0.62 eV.  $\sigma_d$  and  $E_{act}$  turn out to be very insensitive to the SiH<sub>2</sub>Cl<sub>2</sub>/(SiH<sub>2</sub>Cl<sub>2</sub>+SiH<sub>4</sub>) ratio R in the gas phase over the wide range of mixtures R from 0.08 to 0.33. For ratios  $R \geq 0.5$ , the films grow amorphous (Figure 2) and exhibit  $\sigma_d$  values of  $<10^{-12}$  S/cm and  $E_{act}$  of ~1 eV.  $\sigma_{ph}$  of the  $\mu c$ -Si:H film deposited at  $R = 0.08$  is  $2 \cdot 10^{-6}$  S/cm; for films deposited with higher amounts of SiH<sub>2</sub>Cl<sub>2</sub>,  $\sigma_{ph}$  decreases gradually to  $5 \cdot 10^{-7}$  S/cm at  $R = 0.33$ . SiH<sub>2</sub>Cl<sub>2</sub> has the same effect on  $\sigma_d$  and  $E_{act}$  when using the VHF deposition technique, which has been found to be especially favorable to the deposition of  $\mu c$ -Si:H<sup>17</sup>. Values for the VHF-deposited sample at  $R = 0.08$  are  $\sigma_d = 5.4 \cdot 10^{-8}$  S/cm,  $E_{act} = 0.62$  eV and  $\sigma_{ph} = 1.0 \cdot 10^{-5}$  S/cm, the latter being almost an order of magnitude higher than for the best DC-deposited sample.

The growth rate is influenced only slightly by the SiH<sub>2</sub>Cl<sub>2</sub>/(SiH<sub>2</sub>Cl<sub>2</sub>+SiH<sub>4</sub>) ratio and is ~1 Å/s for all samples shown in Figure 1 and Figure 2, which were grown at the power density of ~100 mW/cm<sup>2</sup>. Growth rates of 1.8 Å/s have been obtained by increasing the power density to

$\sim 280 \text{ mW/cm}^2$ . The growth rate for the VHF sample at a power density of  $\sim 45 \text{ mW/cm}^2$  was  $0.8 \text{ \AA/s}$ .

Figure 2 shows the height of the UV reflectance peak at 275 nm, normalized to the peak height for crystalline silicon, as a function of the  $\text{SiH}_2\text{Cl}_2$  fraction. A small amount of  $\text{SiH}_2\text{Cl}_2$  in the plasma is seen to enhance the crystallinity of the film. Upon further increase in  $\text{SiH}_2\text{Cl}_2$ , the crystallinity decreases and eventually the material becomes amorphous at  $R \geq 0.5$ . Raising the temperature enhances the crystallinity (Figure 2), while  $\sigma_d$  and  $E_{\text{act}}$  remain at their intrinsic values of  $\sim 10^{-8} \text{ S/cm}$  and  $>0.6 \text{ eV}$ , respectively. The crystallinity of the VHF-deposited sample is much higher than that of the equivalent DC sample, which explains the slightly higher  $\sigma_d$  at the same  $E_{\text{act}}$  compared to the DC-deposited sample.

Figure 3 shows optical absorption spectra obtained from UV/visible transmission and constant photocurrent method (CPM) spectroscopy. All samples were made at  $R = 0.08$ . Figure 3 features two  $\sim 500 \text{ nm}$  thick films which are deposited using DC excitation at  $210^\circ\text{C}$  and  $280^\circ\text{C}$  and a  $\sim 750 \text{ nm}$  thick VHF-deposited sample ( $210^\circ\text{C}$ ). The absorption spectrum of crystalline silicon is shown for comparison. The sample deposited at the higher temperature has a higher absorption coefficient for red wavelengths. The absorption coefficient in the low-energy region ( $\sim 0.8 \text{ eV}$ ) of the CPM spectrum is an indication of the defect density<sup>18-20</sup>. The absorption coefficient at  $h\nu = 0.8 \text{ eV}$  of the VHF-deposited sample is an order of magnitude lower than that of the DC-deposited sample. This indicates a lower defect density and correlates with  $\sigma_{\text{ph}}$ , which is an order of magnitude higher for the VHF-deposited than for the DC-deposited sample. The CPM spectrum of the VHF-deposited sample is comparable to device-grade  $\mu\text{c-Si:H}$  deposited without  $\text{SiH}_2\text{Cl}_2$ <sup>20</sup>.

Determining the optical bandgap as the intersection of the  $\sqrt{\alpha(h\nu)}$  plot with the energy axis<sup>20</sup>, we obtain a value of roughly 1.1 eV for our  $\mu\text{-Si:H}(\text{:Cl})$  which is the same as the value for  $\mu\text{-Si:H}$  deposited without  $\text{SiH}_2\text{Cl}_2$ <sup>20</sup>. An activation energy of  $\sim 0.6$  eV means that the Fermi level lies close to midgap.

Figure 4 shows a cross-sectional SEM micrograph of the  $\mu\text{-Si:H}(\text{:Cl})$  film deposited at  $R = 0.08$  and using VHF plasma excitation.

#### *Effect of chlorine on oxygen incorporation*

The presence of chlorine in the plasma reduces the oxygen content of  $\mu\text{-Si:H}$ . Figure 5 shows SIMS depth profiles<sup>21</sup> for a sample consisting of three layers of  $\mu\text{-Si:H}$  deposited with three different additions of  $\text{SiH}_2\text{Cl}_2$ . The top and bottom layers are a-Si:H encapsulating layers. Layer A was deposited using only  $\text{SiH}_4$  and  $\text{H}_2$ . The oxygen content  $c_{\text{O}}$  of this layer is as high as  $8 \cdot 10^{19} \text{ cm}^{-3}$ , which explains its high  $\sigma_{\text{d}}$  of  $4.1 \cdot 10^{-3} \text{ S/cm}$  (Figure 1). Layer B was deposited with  $R = 0.08$  at the same  $\text{H}_2$  dilution ratio. In this layer,  $c_{\text{O}}$  is reduced by a factor of two to  $\sim 4 \cdot 10^{19} \text{ cm}^{-3}$ . The chlorine content  $c_{\text{Cl}}$  is  $3\text{-}4 \cdot 10^{19} \text{ cm}^{-3}$ , which is nearly as high as  $c_{\text{O}}$ . For  $R = 0.17$  (layer C),  $c_{\text{O}}$  decreases further to  $3 \cdot 10^{19} \text{ cm}^{-3}$  and  $c_{\text{Cl}}$  increases to  $6\text{-}7 \cdot 10^{19} \text{ cm}^{-3}$ . Chlorine in the plasma therefore reduces  $c_{\text{O}}$  of the growing film whereas the growth rate is nearly unchanged. It is not clear whether the reduction of  $c_{\text{O}}$  can account for the intrinsic character of the films deposited with  $\text{SiH}_2\text{Cl}_2$  or if other mechanisms take place, because  $c_{\text{O}}$  drops by a factor of two upon addition of  $\text{SiH}_2\text{Cl}_2$  whereas  $\sigma_{\text{d}}$  drops by over 5 orders of magnitude.

Figure 6 shows  $c_{\text{O}}$  and  $c_{\text{Cl}}$  in our  $\mu\text{-Si:H}$  for a larger set of samples. The addition of a small amount ( $R = 0.08$ ) of  $\text{SiH}_2\text{Cl}_2$  to the plasma reduces  $c_{\text{O}}$  by over a factor of two. Further additions of  $\text{SiH}_2\text{Cl}_2$  has a smaller effect on  $c_{\text{O}}$ .  $c_{\text{Cl}}$  increases with increasing amount of  $\text{SiH}_2\text{Cl}_2$  in the

plasma. Likewise, we show in Figure 1 that  $\sigma_d$  and  $E_{act}$  of the  $\mu\text{c-Si:H}$  samples made with the smallest addition of  $\text{SiH}_2\text{Cl}_2$  ( $R = 0.08$ ) already correspond to those of intrinsic films.

Possible explanations for the intrinsic character of  $\mu\text{c-Si:H}(\text{:Cl})$  are a) a threshold value of  $c_O$  below which the doping effect of O is negligible, b) the p-type doping effect of Cl compensates the n-type doping of the O, or c) Cl deactivates O as a dopant. Let us briefly discuss these alternatives.

a) O acting as a dopant only above a certain concentration does not seem to be a probable explanation. However, one could imagine that a certain amount of O can be incorporated into the material without creating free carriers and therefore without shifting the Fermi level.

b) Cl has indeed been found to be a slight p-type dopant in a-Si:H<sup>22,23</sup>. However, whereas  $c_{Cl}$  and  $c_O$  are on the same order of magnitude for films deposited with small amounts of  $\text{SiH}_2\text{Cl}_2$ ,  $c_{Cl}$  continues to increase with higher  $\text{SiH}_2\text{Cl}_2$  ratios while  $c_O$  remains almost constant (Figure 6).  $\sigma_d$  would be expected to increase and  $E_{act}$  to decrease with increasing  $c_{Cl}$  if Cl were an efficient dopant.

c) One can imagine that Cl in the material could deactivate the doping effect of oxygen. The number of donors due to the presence of O could indeed be reduced if Si-O- or Si-O-H bonds in “regular”  $\mu\text{c-Si:H}$  were replaced by much stronger Si-O-Cl bonds in  $\mu\text{c-Si:H}(\text{:Cl})$ . At this point it can, however, not be excluded that another reason accounts for the fact that the energetic distribution of defects in  $\mu\text{c-Si:H:Cl}$  differs from that in “regular”  $\mu\text{c-Si:H}$ . The energetic position and charge state of the defect states will determine the position of the Fermi level.

#### *Microcrystalline film growth and oxygen incorporation*

$\sigma_d$  is plotted for a thickness series of  $\mu\text{c-Si:H}$  deposited with  $R = 0.08$  in Figure 7. For very thin films,  $\sigma_d$  corresponds to that of amorphous material. Note that  $\sigma_d$  of a-Si:H deposited with

$\text{SiH}_2\text{Cl}_2$  is usually 1-2 orders of magnitude lower than that of a-Si:H deposited from pure  $\text{SiH}_4$ <sup>24</sup>. Very thin samples are amorphous as the lack of a pronounced UV reflection peak confirms.  $\sigma_d$  and UV reflectance increase within the first 150-200 nm to the final value for bulk  $\mu\text{c-Si:H}$  films. Within approximately the same thickness range, i.e. 100-150 nm, the SIMS hydrogen depth profile shows the transition from a-Si:H to  $\mu\text{c-Si:H}$  with a lower H content (Figure 7, bottom). Interestingly,  $c_{\text{O}}$  also increases only gradually with increasing crystallinity, even though the gas mixture does not change and therefore the amount of O coming with the feedstock gases or from the chamber walls does not change either. We conclude therefore that the altered material structure of  $\mu\text{c-Si:H}$  compared to a-Si:H is the reason for the enhanced O incorporation. The time scale of the increase in the  $c_{\text{O}}$  (~25 min for 150 nm at 1 Å/s) excludes as an explanation O entrained with the feedstock gases and accumulating gradually in the chamber during deposition.

### *Solar cell*

We tested our  $\mu\text{c-Si:H}(\text{:Cl})$  in a solar cell with p-i-n structure (Figure 8). The i-layer thickness is 1.8  $\mu\text{m}$ , the substrate is textured  $\text{SnO}_2$  and the back contact is Ag which was thermally evaporated onto the n-layer, without a ZnO reflector layer in between. The solar cell shows a  $V_{\text{oc}}$  of ~350 mV and red response up to  $\lambda = 1000$  nm (Figure 9). The fill factor is 55 %. Even though the short circuit current density value of 4.14  $\text{mA}/\text{cm}^2$  is low, the flat reverse-bias response suggests that the photo-carrier collection in forward bias is efficient. We believe that non-optimal optical performance (TCO haze, TCO reduction during deposition, lack of back reflector) cause the low photocurrent.



## Conclusions

In conclusion, intrinsic  $\mu\text{c-Si:H}$  can be deposited in a PECVD process when chlorine is present in the plasma. A dark-conductivity of  $5.4 \cdot 10^{-8}$  S/cm, activation energy of 0.62 eV and photo-conductivity of  $1.0 \cdot 10^{-5}$  S/cm are obtained. The optical bandgap for this new material is approximately 1.1 eV. The deposition process does not require any gas purifying or microdoping procedures and is very insensitive to reactor conditions. A small amount of chlorine in the gas enhances the crystallinity of the material and reduces the amount of oxygen incorporated into the sample by over a factor of two. Sub-bandgap absorption spectroscopy indicates a low defect density in our material. VHF deposition yields material with lower defect density and higher photo-conductivity than material deposited using DC plasma excitation. Transition from amorphous to microcrystalline growth happens during the first 100-150 nm of film growth. The altered material structure of  $\mu\text{c-Si:H}$  compared to a-Si:H is the reason for the enhanced O incorporation as the oxygen content increases with increasing crystallinity during growth. A solar cell with a 1.8  $\mu\text{m}$  thick  $\mu\text{c-Si:H}(\text{:Cl})$  i-layer exhibits  $V_{\text{oc}} = 0.35$  V,  $I_{\text{sc}} = 4.14$  mA/cm<sup>2</sup> and FF = 55 %, proving that the material is suitable for device fabrication.

## Acknowledgements

R. Platz thanks the Arthur u. Aenne Feindt Stiftung, Hamburg (Germany), and the Fondation Charles-Edouard Guillaume, Bienne (Switzerland) for funding of his stay at Princeton University. The Electric Power Research Institute supported this research.

## References

- <sup>1</sup> J. Meier, R. Flückiger, H. Keppner, A. Shah, *Appl. Phys. Lett.* 65 (1994) 860.
- <sup>2</sup> J. Meier, S. Dubail, R. Flückiger, D. Fischer, H. Keppner, A. Shah, *Proc. 1st WCPEC* (1994) 409.
- <sup>3</sup> J. Meier, S. Dubail, R. Platz, P. Torres, U. Kroll, J.A. Anna Selvan, N. Pellaton Vaucher, C. Hof, D. Fischer, H. Keppner, R. Flückiger, A. Shah, V. Shklover, K.-D. Ufert, *Solar Energy Materials and Solar Cells* 49 (1997) 35.
- <sup>4</sup> T. Nagahara, K. Fujimoto, N. Kohno, Y. Kashiwagi, H. Kakinoki, *Jpn. J. Appl. Phys.* 31 (1992) 4555.
- <sup>5</sup> S.S. He, G. Lucovsky, *MRS Symp. Proc.* 336 (1994) 25.
- <sup>6</sup> M.W.D. Froggatt, W.I. Milne, M.J. Powell, *MRS Symp. Proc.* 467 (1997) 893.
- <sup>7</sup> S. Veprek, Z. Iqbal, R.O. Kühne, P. Capezutto, F-A. Sarott, J.K. Gimzewski, *J. Phys. C: Solid State Physics* 16 (1983) 6241.
- <sup>8</sup> P. Torres, J. Meier, R. Flückiger, U. Kroll, J.A. Anna Selvan, H. Keppner, A. Shah, S.D. Littlewood, I.E. Kelly, P. Giannoulès, *Appl. Phys. Lett.* 69 (1996) 1373.
- <sup>9</sup> R. Flückiger, J. Meier, M. Goetz and A. Shah, *J. Appl. Phys.* 77(2) (1995) 712.
- <sup>10</sup> F. Wang, H.N. Liu, Y.L. He, A. Schweiger, R. Schwarz, *J. Non-Cryst. Solids* 137&138 (1991) 511.
- <sup>11</sup> Z. Iqbal, P. Capezutto, M. Braun, H.R. Oswald, S. Veprek, G. Bruno, F. Cramarossa, H. Stüssi, J. Brunner, M. Schärli, *Thin Solid Films* 87 (1982) 43.
- <sup>12</sup> H. Shirai, T. Arai and T. Nakamura, *Techn. Dig. PVSEC-9* (1996) 853.
- <sup>13</sup> S.K. Kim, B.Y. Moon, J.S. Byun, H.B. Jeon and J. Jang, *Appl. Phys. Lett.* 69 (1996) 1131.

- <sup>14</sup> A.H. Jayatissa, Y. Nakanishi, Y. Hatanaka, *Jpn. J. Appl. Phys.* 32 (1993) 3729.
- <sup>15</sup> T.I. Kamins, Polycrystalline silicon for integrated circuit applications, Kluwer Academic Publishers 1988, p.68.
- <sup>16</sup> R. Swanepoel, *J. Sci. Instr.* 16 (1983) 1214.
- <sup>17</sup> F. Finger, P. Hapke, M. Luysberg, R. Carius, H. Wagner, M. Scheib, *Appl. Phys. Lett.* 65 (1994) 2558.
- <sup>18</sup> W.B. Jackson, N.M. Johnson, D.K. Biegelsen, *Appl. Phys. Lett.* 43 (1983) 195.
- <sup>19</sup> Z. Iqbal, F.A. Sarott, S. Veprek, *J. Phys. C: Appl. Phys.* 16 (1983) 2005.
- <sup>20</sup> N. Beck, J. Meier, J. Fric, Z. Remes, A. Poruba, R. Flückiger, J. Pohl, A. Shah, M. Vanecek, *J. Non-Cryst. Solids* 198-200 (1996) 903.
- <sup>21</sup> SIMS measurements performed by Evans East, Plainsboro, NJ 08536.
- <sup>22</sup> A.E. Delahoy, R.W. Griffith, *J. Appl. Phys.* 52 (1981) 6337.
- <sup>23</sup> K.S. Lee, J.H. Choi, S.K. Kim, H.B. Jeon, J. Jang, *Appl. Phys. Lett.* 69 (1996) 2403.
- <sup>24</sup> A.M. Payne, B.K. Crone, S. Wagner, *MRS Symp. Proc.* 467 (1997) 789.

Figures

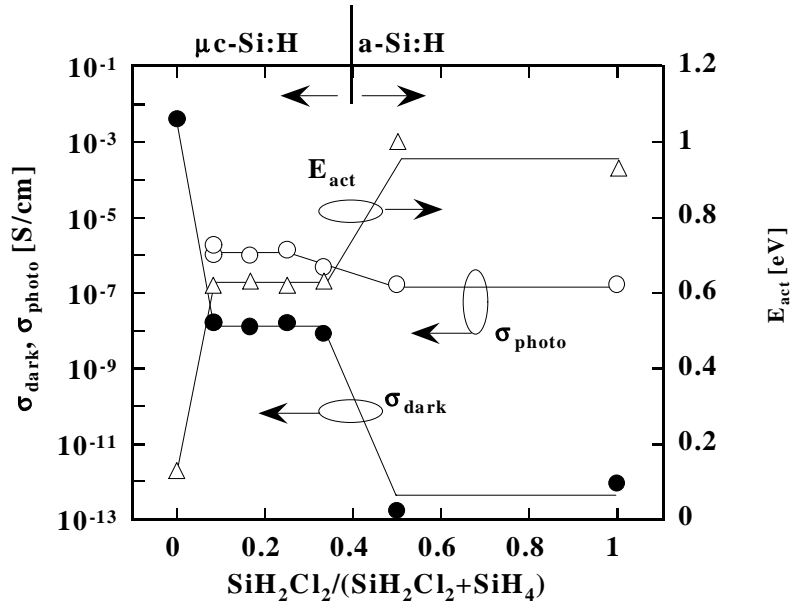


Figure 1

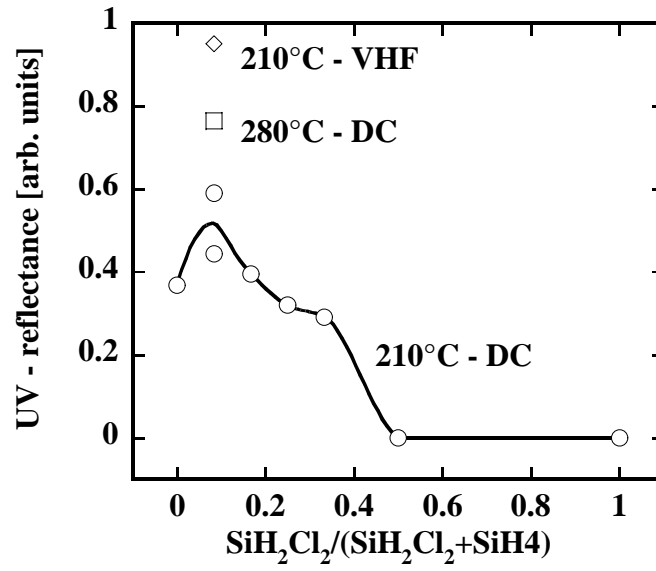


Figure 2

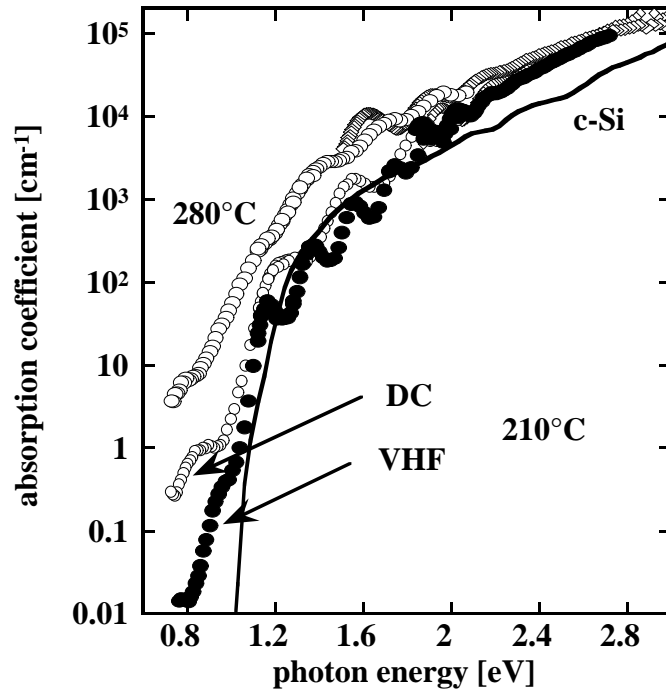


Figure 3

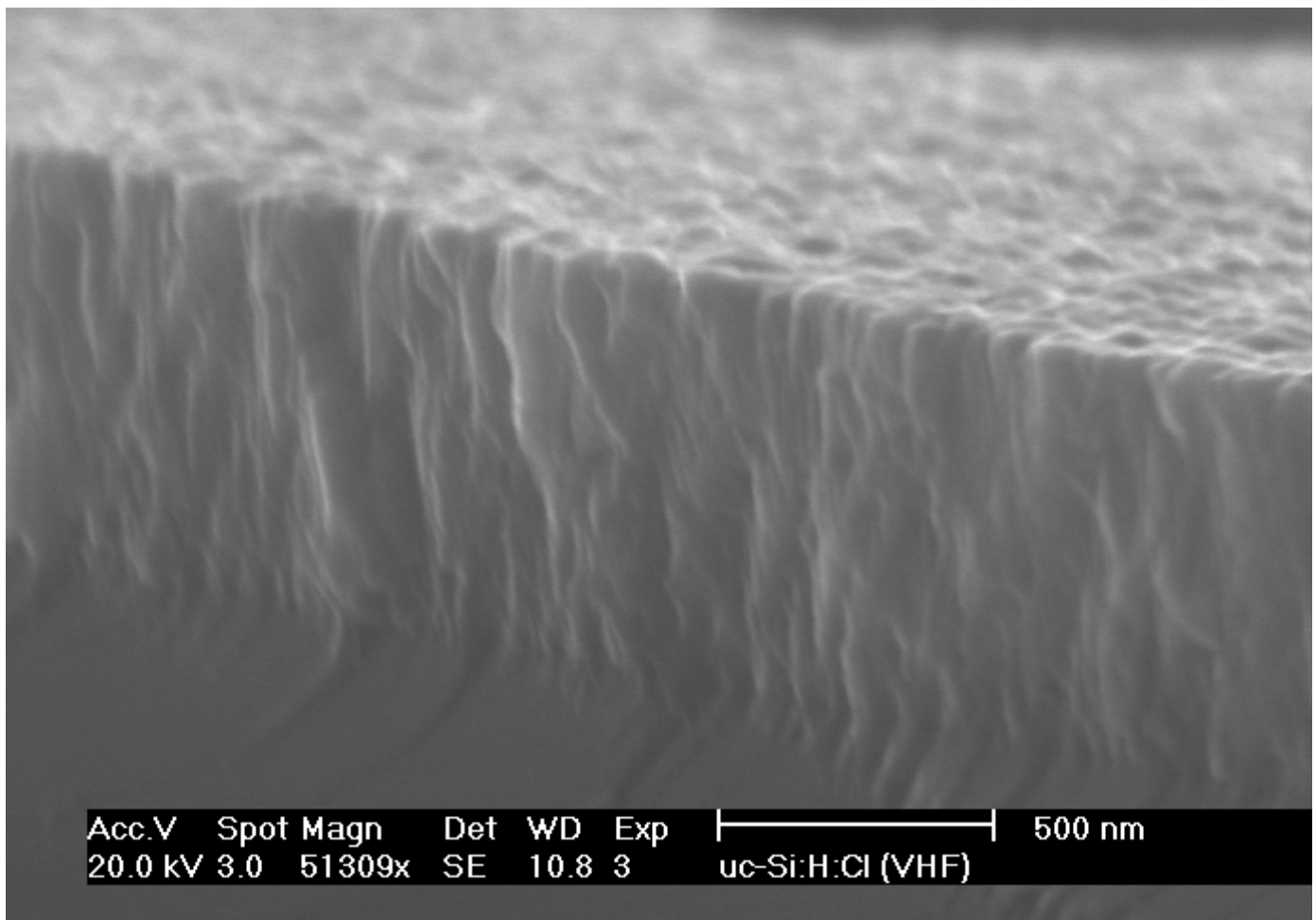


Figure 4

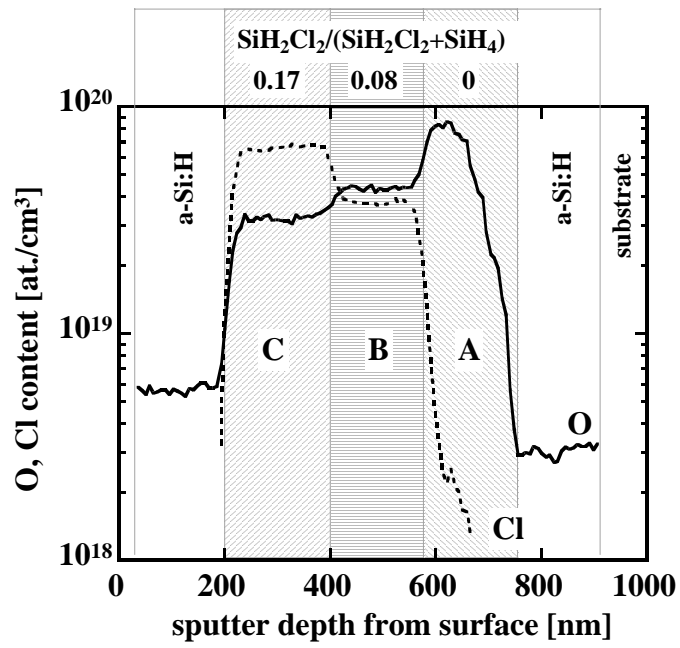


Figure 5



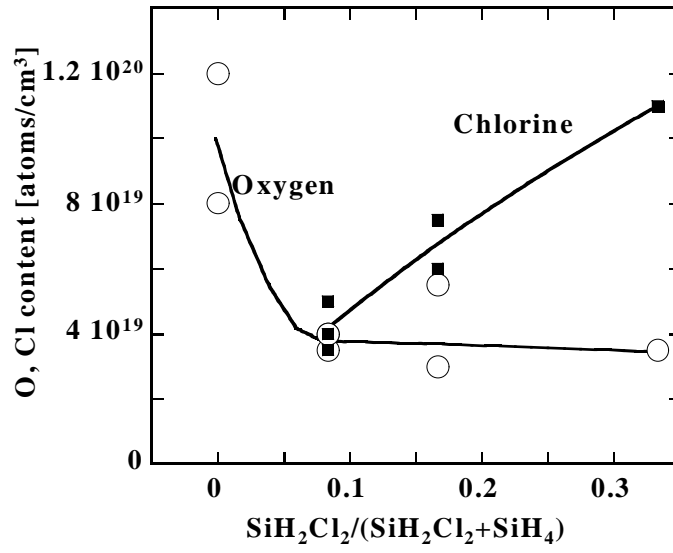


Figure 6

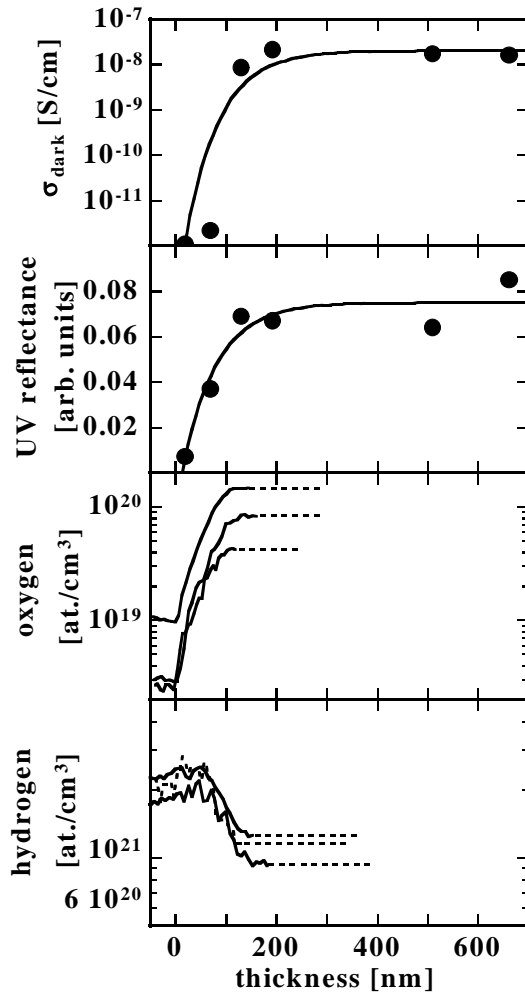


Figure 7

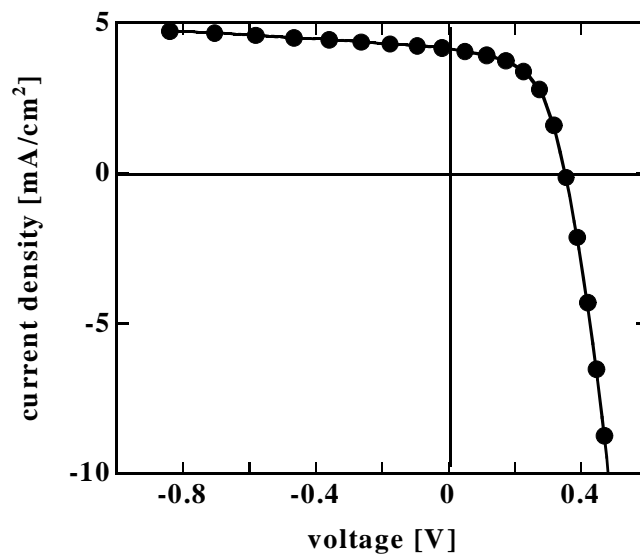


Figure 8

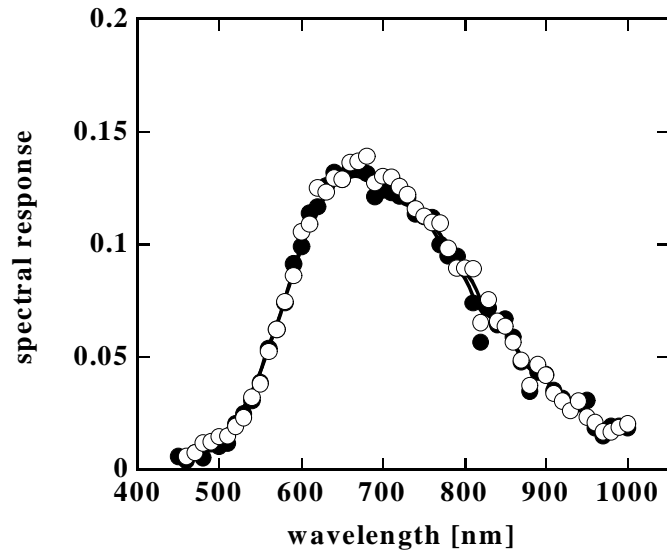


Figure 9

## Figure captions

Figure 1: Dark-conductivity, dark-conductivity activation energy and photo-conductivity as functions of the amount of  $\text{SiH}_2\text{Cl}_2$  in the gas phase for DC-deposited samples.

Figure 2: Ultraviolet reflectance at  $\lambda = 275$  nm normalized to crystalline silicon.

Figure 3: Optical absorption spectra measured by constant photocurrent method (CPM) and UV/visible transmission spectroscopy for two substrate temperatures. Crystalline silicon is shown for comparison.

Figure 4: Cross-sectional SEM micrograph of a VHF-deposited  $\mu\text{c-Si:H}(\text{:Cl})$  film on crystalline silicon substrate.  $\text{SiH}_2\text{Cl}_2$  fraction is  $R = 0.08$ .

Figure 5: Oxygen and chlorine SIMS depth profile for  $\mu\text{c-Si:H}$  deposited on a-Si:H and capped with a-Si:H. The  $\mu\text{c-Si:H}$  layers were deposited with  $\text{SiH}_2\text{Cl}_2/(\text{SiH}_2\text{Cl}_2+\text{SiH}_4)$  ratios of 0 (layer A), 0.08 (B), and 0.17 (C). Note the opposite trends in Cl and O concentrations. All layers are deposited using DC plasma excitation.

Figure 6: Oxygen and chlorine content in our  $\mu\text{c-Si:H}$  as a function of the  $\text{SiH}_2\text{Cl}_2$  ratio. All layers are deposited using DC plasma excitation.

Figure 7: Top: dark-conductivity and UV reflectance for a thickness series of  $\mu\text{c-Si:H}$  deposited with a  $\text{SiH}_2\text{Cl}_2 / (\text{SiH}_2\text{Cl}_2+\text{SiH}_4)$  ratio of 0.08 in a DC-excited plasma. Bottom: oxygen and hydrogen depth profiles from SIMS for  $\mu\text{c-Si:H}$  samples deposited with and without  $\text{SiH}_2\text{Cl}_2$  in the plasma. The figure shows the transition from amorphous to microcrystalline silicon within the first 150 nm of growth. This transition and the increase in the oxygen content occur simultaneously.

Figure 8: I-V curve of a p-i-n solar cell with an i-layer of 1.8  $\mu\text{m}$  thick  $\mu\text{c-Si:H}(\text{:Cl})$  deposited by VHF.

Figure 9: Spectral response of the solar cell of Figure 8 measured at 0 V ( $I_{\text{sc}}$  conditions, black symbols) and -2 V (open symbols) bias.